Available online at www.sciencedirect.com
ScienceDirect
International Journal of Mass Spectrometry 270 (2008) 8–15
International Journal of Mass Spectrometry
www.elsevier.com/locate/ijms

Calibration of a frequency-scan quadrupole ion trap mass spectrometer for microparticle mass analysis

Zongxiu Nie [a,b], Fenping Cui [a,c], Minglee Chu [d], Chung-Hsuan Chen [e], Huan-Cheng Chang [a,e,*], Yong Cai [f,**]

[a] *Institute of Atomic and Molecular Sciences, Academia Sinica, Taipei 106, Taiwan*
[b] *Department of Physics, Wuhan University, Wuhan 430072, China*
[c] *College of Mathematics and Physics, Nanjing University of Information Science and Technology, Nanjing 210044, China*
[d] *Institute of Physics, Academia Sinica, Taipei 115, Taiwan*
[e] *Genomics Research Center, Academia Sinica, Taipei 115, Taiwan*
[f] *Department of Atmospheric Science, University of Wyoming, Laramie, WY 82071, United States*

Received 30 August 2007; received in revised form 16 October 2007; accepted 26 October 2007
Available online 9 November 2007

Abstract

Charge detection quadrupole ion trap (QIT) mass spectrometry (MS) is a promising technique for high-speed mass analysis of micron-sized particles such as biological cells and aerosols. In this technique, the trap can be conveniently operated in the mass-selective axial instability mode by scanning the frequency of the applied ac field under a low vacuum condition. However, because of the lack of proper mass standards in the m/z range of 10^9, a method of calibrating both the resolution and measurement accuracy of the mass spectrometer is required. Herein, we describe a calibration method which involves determination of the points of ejection (q_{eject}) of the individual particles to be analyzed and investigating how these q_{eject} points vary with the trap imperfection, the frequency-scan range, the scan speed, and the pressure of buffer gas. The results are compared with theoretical simulations based on the generalized nonlinear Mathieu equations. Using NIST polystyrene size standards as the test samples, we determined a mean ejection point of $q_{eject} = 0.952$ at the trap driving voltage amplitude of 1617 V, a He buffer gas pressure of 40 mTorr, and a frequency-scan rate of 70 Hz/s over the scan range of 450–100 Hz. The coefficient of variance of the measured q_{eject} points is 1.2%, suggesting that a resolution of ∼100 and a measurement accuracy of ∼1% can be achieved after careful calibration of the frequency-scan QIT mass spectrometer.

Keywords: Quadrupole ion trap; Charge detection; Frequency scan; Microparticles

1. Introduction

Quadrupole ion trap (QIT) has been widely used as a mass analyzer since its invention by Paul et al. [1] and concurrently by Wuerker et al. [2] in the late 1950s. The device is robust, compact, and capable of providing high mass resolution when operating in the mass-selective axial instability mode [3–5]. Being an ion storage device, it has also been utilized as an electrodynamic balance for absolute mass determination of micron-sized particles such as aerosols [6] and synthetic polymers [7]. It is one of the most versatile mass analyzers available in the field.

When using the QIT as a microparticle balance, the frequency of the ac field applied to the ring and/or endcap electrodes is typically in the range of 1 kHz or less. Because of this low frequency, in order to achieve high mass measurement accuracy (better than 1%), only one particle is analyzed at a time over a time period of seconds up to minutes [8–13]. This long detection time, however, prevents the technique from routine and practical applications. A previous study [14,15] has shown that it is possible to integrate the mass-selective axial instability mode with the QIT for high-speed mass analysis of microparticles using light scattering as a detection method. A recent experiment [16] demonstrated that these particles can be detected by using an image charge detection plate which, additionally, provides a direct measure of the absolute number of the charges carried by the particles. This

* Corresponding author at: Institute of Atomic and Molecular Sciences, Academia Sinica, Taipei 106, Taiwan.
** Corresponding author.
E-mail addresses: hcchang@po.iams.sinica.edu.tw (H.-C. Chang), ycai@uwyo.edu (Y. Cai).

1387-3806/$ – see front matter © 2007 Elsevier B.V. All rights reserved.
doi:10.1016/j.ijms.2007.10.012

newly developed technology has been successfully applied to measure the total dry masses and associated mass distributions of synthetic polymeric microparticles, cancer cells [16] and red blood cells [17].

In operating the QIT in the mass-selective axial instability mode, ramping up the ac voltage amplitude at a constant frequency is an effective approach, while ramping down the trap driving frequency at a constant voltage amplitude is the other [18]. The advantage of the latter is that the trap can be operated under mild vacuum conditions (pressure ~10 mTorr) without arcing between the ring and endcap electrodes. This is an important feature since it has been demonstrated [10–12,14,15] that gas damping is an effective means in reducing the total kinetic energy of the ionized microparticles produced by either electrospray ionization, matrix-assisted laser desorption/ionization, or laser-induced acoustic desorption (LIAD) for trapping. Evidence has also been found that the presence of buffer gas assists detection of the charged particles ejected from the QIT [16,17].

The feasibility of operating the QIT in the frequency-scan mode for analysis of high-mass biomolecules was first demonstrated by Schlunegger et al. [19]. The authors swept the trap driving frequency from 30 kHz to 10 kHz at a constant voltage amplitude of 200 V, and successfully obtained the mass spectra of singly charged IgG at $m/z \approx 1.5 \times 10^5$ with a mass resolution approaching 100. However, the difficulty in electronics hampered the operation of the frequency-scan QIT over a wider frequency range. The situation worsened when extending the study to larger biomolecules or bioparticles (such as viruses) since no suitable detector was available [7]. Very few work on the frequency-scan QIT-MS was reported since then, except those from our groups [16,17,20,21] and the Shimadzu group [22–25] working on digital ion traps.

This study was motivated by our recent development of charge detection QIT-MS for high-speed mass analysis of biological cells evaporated/ionized by LIAD [16,17]. In this analysis, in order for the cells to be effectively captured by the QIT and subsequently detected by the charge detection plate, the typical He buffer gas pressure used was in the range of 40 mTorr or higher. Because of this high pressure, it is crucial for the spectrometer to be operated in the frequency-scan mode so that the trap driving voltage can be maintained below the arcing threshold of the electrodes. However, it has been an open and important question how the buffer gas affects the ion ejection process at high pressures [26,27]. A method for calibrating the resolution and the measurement accuracy of the mass spectrometer, together with the sensitivity of the charge-sensitive detector, is thus required.

We have previously developed a method to calibrate the QIT operating in the voltage scan mode for mass analysis of microparticles [15]. Results of the calibration showed that the mass analyzer, a standard unstretched QIT, used in our experiment was imperfect. The trap imperfections may come from truncation of the hyperbolic electrodes, drilling of holes on the electrode assemblies, machining inaccuracy, as well as any possible misalignments between the ring and the endcap electrodes. Although there is a lack of mass standards in the m/z range of 10^9, both the resolution and measurement accuracy of this mass spectrometer can be properly characterized by a self-calibration method [15]. It involves high-precision measurement of the axial secular frequency (hence, its m/z) of a single particle inside the QIT, followed by monitoring the action of the ejection of this particle in real time to determine the point of ejection (q_{eject}). This work adopts the same method with the exception that the QIT is now operated in the frequency-scan mode. From a systematic measurement of more than 100 particles, a mean value of the measured q_{eject} and its distribution width were obtained. The results are compared closely with theoretical simulations based on the generalized Mathieu equations which take the gravity, the buffer gas damping effect, and the nonlinearity of the trapping field all into account.

2. Methods

2.1. Theory

The method of calibrating the QIT mass spectrometer consists of two parts. First, we characterize carefully the parameter β_z as a function of q_z near the boundary ($\beta_z = 1$) of the stability diagram of the QIT at $a_z = 0$ using a single trapped particle. For the QIT operating in the monopolar mode, either the ring electrode is grounded or the two endcap electrodes are grounded as employed herein, the two trap parameters are defined as [18]

$$\beta_z = \frac{2\omega_z}{\Omega} \tag{1}$$

and

$$q_z = \frac{4ZeV_{\text{ac}}}{mr_0^2\Omega^2}, \tag{2}$$

where ω_z is the axial secular frequency, Ω is the trap driving frequency, Z is the number of charge, e is the elementary charge, V_{ac} is the trap driving voltage amplitude (i.e., zero-to-peak voltage), m is the ionic mass and r_0 is the radius of the ring electrode. For an ideal QIT, $q_{\text{eject}} = 0.908$ at $\beta_z = 1$; however, this point may shift due to the trap imperfections [28]. We determine the value of β_z directly from a measurement of ω_z for a single charged particle oscillating inside the trap according to Eq. (1) and calculate the mass-to-charge ratio of this particle at $\beta_z \leq 0.2$, where the pseudo-potential approximation [18,29]

$$\beta_z = \frac{q_z}{\sqrt{2}} \tag{3}$$

applies as [2,29]

$$\frac{m}{Ze} = \frac{\sqrt{2}V_{\text{ac}}}{r_0^2\Omega\omega_z}. \tag{4}$$

With this m/Ze the q_z value at given r_0, Ω and V_{ac} can be calculated from Eq. (2) accordingly. A plot of β_z versus q_z can be therefore derived from repeated measurements of ω_z at various Ω over the range of $\beta_z = 0$–1 for the same particle (i.e., with the same m/Ze). Fig. 1 shows a typical result of such measurements.

Second, we monitor the action of the particle ejection in real time when the trap driving frequency is ramped down. From the measured ejection frequency (Ω_{eject}), the q_{eject} value of

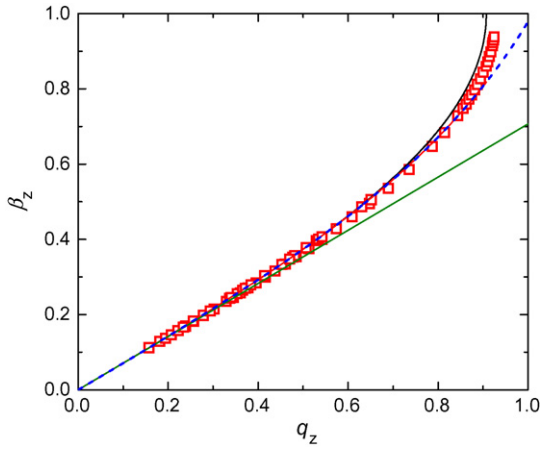

Fig. 1. Plot of β_z versus q_z along the $a_z = 0$ axis of the Mathieu stability diagram for the three-dimensional quadrupole ion trap. Red open squares are the experimental values obtained from repeated measurements of ω_z at various Ω for the same particle (see text for details). The black solid curve is the result calculated from the continued fractions of β_z as a function of q_z for an ideal quadrupole ion trap [18], and the blue dashed curve and the green solid line are calculated results using Eqs. (5) and (3), respectively. (For interpretation of the references to color in this figure legend, the reader is referred to the web version of the article.)

the particle (with a prior measured ω_z) is calculated from Eq. (2). The q_{eject} so determined is a combined result of the ejection delay due to the trap imperfection, the buffer gas damping (40 mTorr of He in the present case), as well as the detection delay due to the finite scan time (typically 5 s). To assess the degree of the detection delay, which can be prominent for the QIT operating in the frequency-scan mode, we systematically measure the dependence of q_{eject} on the frequency-scan rate. The buffer gas damping effect is also evaluated from a pressure dependence measurement. In this part of the experiment, a more general approach (not limited to $\beta_z \leq 0.2$ or $q_z \leq 0.3$) is taken to determine *m/Ze* from the measured ω_z for each particle. Mathematically, it has been shown that [30]

$$\beta_z \approx \sqrt{\frac{q_z^2}{2 - q_z^2} - \frac{7}{128}q_z^4 + \frac{29}{2304}q_z^6}, \tag{5}$$

which is valid up to $q_z = 0.7$ with a deviation of <1% from the exact value (Fig. 1). Combining Eqs. (1), (2), (5) and expressing β_z as a polynomial of q_z yield [11]

$$\frac{2\omega_z}{\Omega} = \frac{1}{\sqrt{2}}\left[C\left(\frac{4\pi^2 V_{\text{ac}}}{\Omega^2}\right) + \frac{25C^3}{128}\left(\frac{4\pi^2 V_{\text{ac}}}{\Omega^2}\right)^3 + \frac{34,951C^5}{294,912}\left(\frac{4\pi^2 V_{\text{ac}}}{\Omega^2}\right)^5 - \frac{7925C^7}{294,912}\left(\frac{4\pi^2 V_{\text{ac}}}{\Omega^2}\right)^7 - \frac{100,489C^9}{10,616,832}\left(\frac{4\pi^2 V_{\text{ac}}}{\Omega^2}\right)^9\right], \tag{6}$$

where the parameter C is defined as

$$C = \frac{Ze}{mr_0^2\pi^2}. \tag{7}$$

Fitting of the experimental data (including ω_z, Ω and V_{ac}) to Eq. (6) allows us to determine precisely the C parameter or the *m/Ze* value of the particle. The particle ejection point q_{eject} can finally be calculated from Eq. (2) as

$$q_{\text{eject}} = \frac{4\pi^2 V_{\text{ac}} C}{\Omega_{\text{eject}}^2}, \tag{8}$$

where Ω_{eject} is the frequency at which the particle is ejected from the QIT.

2.2. Experiment

The sample used in this experiment was the NIST polystyrene size standard, SRM 1692. The certified number-averaged diameter of the spheres is 2.982 μm, with a standard deviation of 0.016 μm. Use of the density of 1.055 g/cm^3 for polystyrene [31] leads to a calculated mean mass of 8.81×10^{12} Da/particle. It is noted that the coefficient of variance (CV) of the mass distribution of this sample is only 1.6%. This narrow mass distribution suggests that the NIST polystyrene size standards are useful as the mass standards in particle mass spectrometry [11].

The experimental setup employed in this work is generally similar to that reported previously by Cai et al. [14,15]. Specifically, the QIT was obtained from Jordan TOF Products (Grass Valley, CA, USA) and has an unstretched geometry of $r_0 = 10$ mm and $z_0 = 7.07$ mm, where r_0 is the radius of the ring electrode and z_0 is half the distance between the two endcap electrodes. Compared to the earlier work, four major modifications have been made to widen the biological application of this mass spectrometer. First, a LIAD source was used to evaporate charged microparticles from a silicon substrate without matrix and external ionization [11,12]. Second, the evaporated particles entered the ion trap through one of the four holes on the ring electrode [17]. Third, a small ac voltage was applied between the two endcap electrodes for resonance ejection of the trapped particles until one was left for secular frequency measurement [17]. Fourth, a home-built charge-sensitive plate detected the particles ejected from one of the endcaps of the QIT [16,17]. Further experimental details can be found in refs. [15,17].

Trapping of the LIAD-generated particles was performed in the presence of 40 mTorr of He buffer gas. More than one particle was often trapped in each filling. To achieve single particle trapping, the chamber was first evacuated to a base pressure of less than 1 mTorr and unwanted particles were eliminated consecutively by resonance ejection. A He–Ne laser beam illuminated the selected particle for visual monitoring of its oscillatory motions inside the QIT. Observation of a stable 2:1 Lissajous trajectory ensured trapping of a single particle. Secular frequencies of the particle's oscillation were determined by performing a fast Fourier transform of the monitored, intensity-modulated light signals [9,10]. An accuracy on the order of $\Delta\omega_z/\omega_z = 10^{-3}$ was readily achievable in a 10-s measurement. After the secular frequency measurement, the chamber was backfilled with 40 mTorr of He buffer gas right before ejection of the trapped particle for *m/z* analysis. Experiments with no backfilling of the chamber with the He gas were also conducted for comparison.

A key component that made possible operation of the QIT-MS in the frequency-scan mode was the high-voltage current-feedback power amplifier built in house [32].[1] The amplifier was so well designed that the variation of V_{ac} with Ω was less than 1% over the frequency-scan range of 100–1000 Hz. In addition to this power amplifier, a high-precision averaging peak-to-peak voltage detector [33] was also developed to measure precisely the V_{ac} value throughout the entire experiment. Use of this home-built peak-to-peak voltage detector, which was calibrated against a standard voltage and frequency source, has allowed us to achieve high-precision measurement for the ac voltage amplitude at the level of 100 ppm.

3. Results and discussion

3.1. Experimental results

Fig. 1 depicts a plot of β_z versus q_z, obtained from the experimentally measured ω_z at $V_{ac} = 1617$ V and $\Omega/2\pi = 610$–267 Hz in vacuum (chamber base pressure <1 mTorr). Each data point is a result of the measurement for the axial secular frequency at a different trap driving frequency. No gravitational effects were taken into account in this measurement since the gravity has been shown to play no significant role here [34], particularly near the particle ejection point. As shown in Fig. 1, the data points match closely with the theoretical values obtained from successive approximation of β_z as a function of q_z [18] for an ideal ion trap at $q_z < 0.5$. However, as q_z approaches to 0.9, clear deviation between experiment and theory is found. Extrapolation of the experimental data to the stability diagram boundary of $\beta_z = 1$ suggests an ejection point of $q_{eject,0} = 0.935$. The value is in excellent agreement with our previous measurement where V_{ac} was varied [15]. Again, the value is significantly larger than 0.908, a result that the QIT used in this experiment is imperfect because of the presence of multipole components in the trapping potential [15].

The $q_{eject,0} = 0.935$ attained above is the value determined under a static condition, that is, the scan of the ac frequency is infinitely slow. This operation, however, is impractical in real-world applications. To determine the particle ejection point more directly (or realistically), we ramped down the trap driving frequency (typically in 5 s) and monitored the ejection action of the particle with a pre-determined m/Ze in real time. From the Ω_{eject} detected in the frequency-scan spectrum, the q_{eject} was calculated from Eq. (8). Fig. 2 shows a result of the measurement for the 3-μm NIST spheres in the absence of buffer gas. In this measurement, the trap was operated in the frequency range of 450–100 Hz at a linear scan rate of $\Delta(\Omega/2\pi)/\Delta t = 70$ Hz/s, and the ac voltage was maintained at a constant amplitude of $V_{ac} = 1617$ V. Eleven particles were measured individually and they all carried different numbers of charges and therefore were ejected at different frequencies. We determined a mean ejection point of $q_{eject} = 0.947$ with a CV of 1.2%. Compared with $q_{eject,0} = 0.935$ as determined earlier in the static condition, the

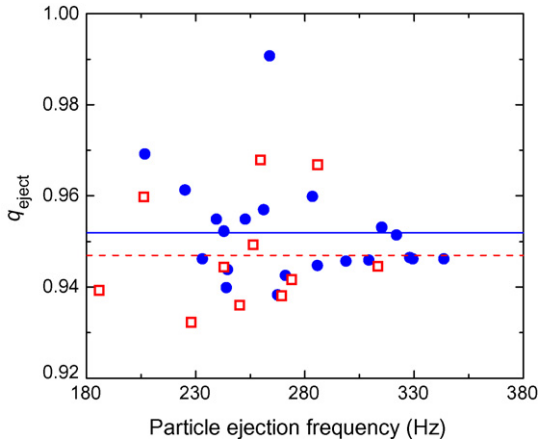

Fig. 2. Single particle measurements of q_{eject} with (●) and without (□) 40 mTorr of He buffer gas. Both the measurements were conducted at the frequency-scan rate of 70 Hz/s, the frequency-scan range of 450–100 Hz, and the ac voltage amplitude of 1617 V. The mean values of these two data sets are $q_{eject} = 0.947$ (dashed line) and $q_{eject} = 0.952$ (solid line), respectively.

delay in particle ejection here is more prominent. To confirm that the additional delay (∼1%) is a result of the delay in particle detection due to the finite scan time, we measured systematically how q_{eject} varies with the frequency-scan rate.

Fig. 3 shows the result of the q_{eject} measurement at four different frequency-scan rates in the absence of buffer gas. As seen, the measured q_{eject} increased nearly linearly with the rate when the frequency was swept over the same range of 450–100 Hz. Accompanied with this increase is the increase of the CV in q_{eject}. The CV has more than tripled as the rate increased from 35 Hz/s to 350 Hz/s, a reflection that the mass resolution of the spectrometer is lower at higher frequency-scan rates. Extrapolating the data points to the zero scan rate yields an intrinsic ejection point of $q_{eject,0} = 0.935$ with a CV of only ∼1%. The former is in excellent agreement with the value $q_{eject,0} = 0.935$ determined earlier (Fig. 1) within the limit of our experimental errors (∼1%). Note that the CV measured here is twice as large

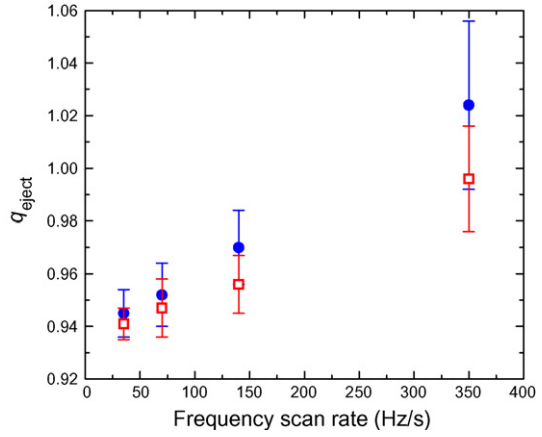

Fig. 3. Dependence of experimentally measured q_{eject} on the frequency-scan rate with (●) and without (□) 40 mTorr of He buffer gas. Both the experiments were conducted at the frequency-scan range of 450–100 Hz and the ac voltage amplitude of 1617 V. Extrapolating the data points of these two measurements to the zero scan rate yields the same ejection point of $q_{eject,0} = 0.935$.

[1] Detailed information of the circuit is available upon request.

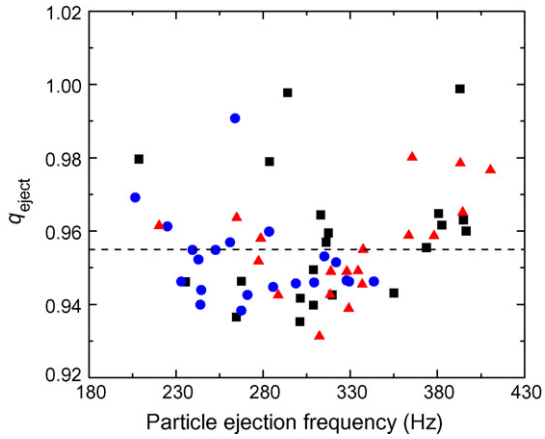

Fig. 4. Single particle measurements of q_{eject} at the trap driving voltages of V_{ac} = 1500 V (▲), 1617 V (●) and 1815 V (■). The measurements were conducted in the presence of 40 mTorr of He buffer gas with a frequency-scan rate of 70 Hz/s over the range of 450–100 Hz. Note that the data collected at 1617 V here are the same as those shown in Fig. 2. The black dashed line represents the mean value (0.955 ± 0.015) of all q_{eject} measured at the three different voltage amplitudes.

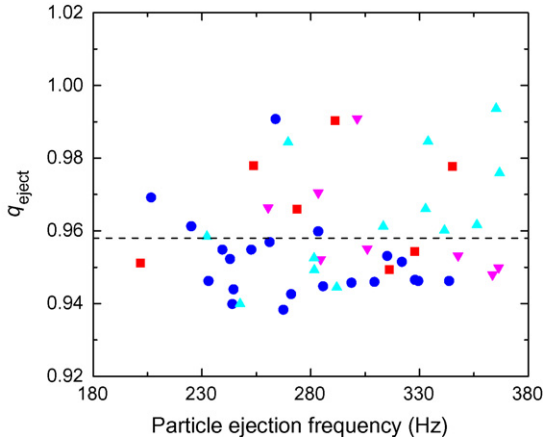

Fig. 5. Single particle measurements of q_{eject} with the trap driving frequency scanned over the ranges of 400–100 Hz (▲), 450–100 Hz (●), 500–100 Hz (■) and 550–100 Hz (▼). The measurements were conducted in the presence of 40 mTorr of He buffer gas at a constant ac voltage amplitude of 1617 V and a frequency-scan rate of 70 Hz/s. The black dashed line represents the mean value (0.958 ± 0.015) of all q_{eject} measured at the four different frequency-scan ranges.

as that (CV ∼ 0.5%) of the voltage scan [15]. It indicates that the particle ejection point is less stable in the frequency-scan mode than in the voltage scan mode. Nonetheless, the result of the present measurement strongly suggests that a resolution of 100 can potentially be reached at $m/z \sim 10^9$ by the frequency-scan QIT-MS.

Aside from the detection delay, the buffer gas damping effect also plays an important role in shifting the q_{eject} point. Shown in Fig. 3 are the results of the measurement in the presence of 40 mTorr of He buffer gas, a typical condition used in the cell experiment [17]. The measured ejection point is fairly stable; it has a mean value of q_{eject} = 0.952 (CV = 1.2%), noticeably higher than its counterpart (q_{eject} = 0.947) by 0.005 unit (cf. Fig. 2). However, the difference is within the distribution width of the measured q_{eject}, indicating that the buffer gas damping effect is small (if not negligible) when the QIT was operated in the frequency-scan mode at the frequency-scan rate of 70 Hz/s. To further investigate the stability of the particle ejection point in the presence of buffer gas, we measured the variation of q_{eject} with the amplitude of the ac field applied to the ring electrode. The result is shown in Fig. 4. As seen, both the measured mean value and the CV of the q_{eject} distribution are insensitive to the changes of the applied voltages, as along as the voltage amplitude was maintained as a constant over the entire frequency-scan range. Similarly, the change is insignificant if the frequency-scan range was varied to 550–100 Hz and 400–100 Hz (Fig. 5).

The present measurement using NIST polystyrene size standards as the test sample provides not only a means to calibrate the QIT mass spectrometer but also a means to calibrate the sensitivity of the charge detector. In the charge detection scheme as employed in this experiment, the measured voltage is converted from the image charges integrated over a small capacitor in the circuit. Since the capacitance (1 pF in this case) of this capacitor has a marked tolerance of ±25%, it introduces a fixed error in the charge measurement. With use of the NIST polystyrene spheres as the mass calibrant, we are allowed to alleviate this problem and determine quite accurately the absolute number of the charges carried by each particle to a precision of better than 2%. Fig. 6 shows the typical charge distribution of the particles investigated in this work. A nearly equal population of both positively and negatively charged particles was detected, a result consistent with the characteristics of LIAD [12]. Further improvement of the charge measurement accuracy relies on increasing the charge number Z or decreasing the electronic noise (typically 500 electron charges [16,17]) of the detector.

3.2. Theoretical simulations

The value $q_{eject,0}$ = 0.935 determined in the experimental sections indicates that the ion trap used in this work is nonlinear. The

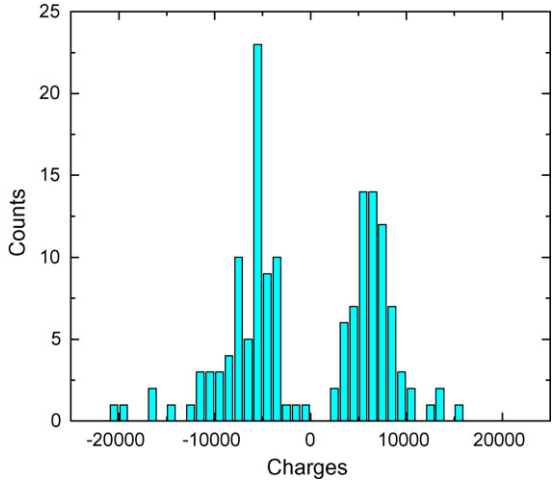

Fig. 6. Charge state distribution of 3-μm polystyrene size standards evaporated/ionized by laser-induced acoustic desorption and captured by the quadrupole ion trap operating in the frequency range of 400–550 Hz and the voltage amplitude range of 1500–1815 V.

nonlinearity may derive from the octopole term in the electric potential [35–38]

$$V(r,z,\phi) = A_2\left[\frac{V_0}{2r_0^2}(r^2-2z^2)\right] + A_4\left[\frac{V_0}{8r_0^4}(8z^4-24z^2r^2+3r^4)\right], \quad (9)$$

where V_0 is the potential applied to the ion trap electrodes. We have previously shown [15] that inclusion of the octopole term with the polarity and magnitude of $A_4/A_2 = -3\%$ can properly reproduce our experimental observation of $q_{\text{eject},0} = 0.935$ at $\Omega/2\pi = 300$ Hz. Based upon this finding, we simulated numerically the present experimental results (obtained by the frequency scan) using the nonlinear Mathieu equations after taking into account the effects of the gravity and the aerodynamic drag force [39,40] on the particle at $a_x = a_y = a_z = 0$ (i.e., no dc fields [18]) as follows

$$\frac{d^2x}{d\xi^2} + b\frac{dx}{d\xi} - 2q_x\left(x - \frac{A_4}{A_2}\frac{\partial V'}{\partial x}\right)\cos 2\xi = 0, \quad (10)$$

$$\frac{d^2y}{d\xi^2} + b\frac{dy}{d\xi} - 2q_y\left(y - \frac{A_4}{A_2}\frac{\partial V'}{\partial y}\right)\cos 2\xi = 0, \quad (11)$$

$$\frac{d^2z}{d\xi^2} + b\frac{dz}{d\xi} - 2q_z\left(z + \frac{A_4}{2A_2}\frac{\partial V'}{\partial z}\right)\cos 2\xi = \frac{4g}{\Omega^2}, \quad (12)$$

where

$$\xi \equiv \frac{\Omega t}{2}, \quad (13)$$

$$V'(r,z,\phi) \equiv \frac{1}{8r_0^2}(8z^4 - 24z^2r^2 + 3r^4), \quad (14)$$

and g is the gravitational acceleration on Earth surface and b is the gas damping parameter, which is related to the buffer gas pressure (p), the molar weight (M) and temperature (T) of the buffer gas atoms (or molecules), as well as the density (ρ_0) and diameter (d) of the investigated particle by [41]

$$b = \frac{8.6p}{\rho_0 d\Omega}\sqrt{\frac{M}{RT}}. \quad (15)$$

Use of the parameters $d = 2.982\,\mu$m, $\rho_0 = 1.055$ g/cm^3, $p = 4\times10^{-2}$ Torr, $M = 4$ g/mol and $T = 300$ K yields a unitless number $b \approx 0.01$ at $\Omega/2\pi = 450$ Hz. It should be emphasized that the parameter b here is no longer a constant in the frequency-scan mode. It is inversely proportional to Ω and, hence, increases continuously as the frequency is ramped down. Another noteworthy complication in the frequency-scan simulation is that the motion of the ions in the QIT is a function of both frequency and time. As a result, the ion motion is highly sensitive to the phase of the sinusoidal wave used in the simulation, which often leads to minor fluctuations of q_{eject} and eventually produces erroneous q_{eject} values, if the precision used in the numerical calculation is not sufficiently high.

Fig. 7 shows the results of the simulations for two different cases, (a) $A_4/A_2 = -3\%$ and $b = 0$ and (b) $A_4/A_2 = -3\%$ and $b = 0.01$ at the starting frequency. It illustrates how the particle's position varies with time in the z direction when the trap driving frequency is ramped down from 450 Hz to 100 Hz at $V_{\text{ac}} = 1617$ V. In this simulation, the initial conditions used were ($x_0 = 0$, $\upsilon_{x,0} = 0$), ($y_0 = 0$, $\upsilon_{y,0} = 0$) and ($z_0 = 1$ mm, $\upsilon_{z,0} = 0.01$ m/s), where υ_x, υ_y and υ_z are the velocities of the particles in the x, y and z coordinates, respectively. Due to the gravity, the particle has a small displacement from the trap center ($x = y = z = 0$). We set the starting point arbitrarily at $q_z \sim 0.4$. At this point, a 3-μm polystyrene sphere would carry about 4500 charges in the trap operating at $V_{\text{ac}} = 1617$ V and $\Omega/2\pi = 450$ Hz. As clearly seen in Fig. 7b, the particle stayed at a site very close to the trap center (within 0.1 mm) over a wide range of $q_z = 0.5$–0.9. As q_z increases beyond 0.9, the particle's motion becomes unstable and the oscillation amplitude enlarges exponentially with time. Compared with the voltage scan as discussed in ref. [15], the frequency scan here produces a significantly faster increase in amplitude near the particle ejection point, which can be understood as a result of the quadruple increase of q_z with the decreasing Ω. It is worth noting that the particles so ejected have a velocity of $\upsilon \approx z_0\Omega_{\text{eject}}/2$ [21]. Taking particles ejected at $\Omega_{\text{eject}}/2\pi = 300$ Hz as an example, they have a velocity of 6.7 m/s, which translates to a total kinetic energy of 2 MeV for the 3-μm polystyrene sphere.

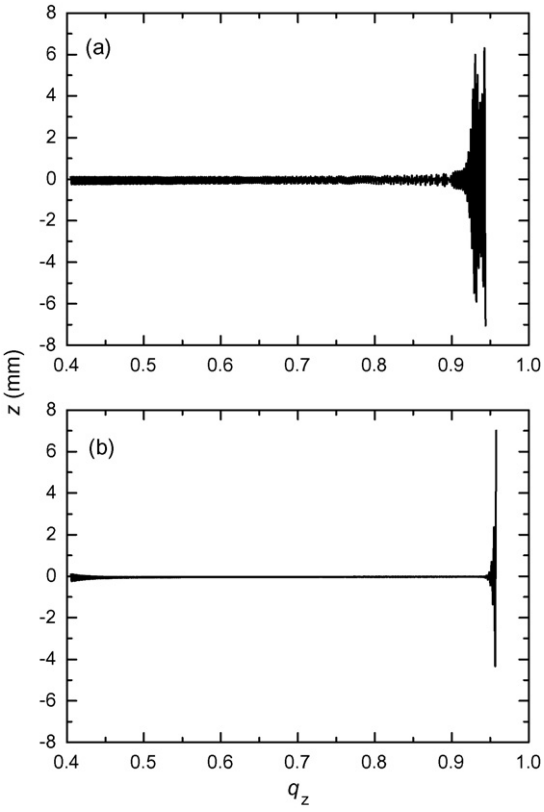

Fig. 7. Variations of the particle position z with the trap parameter q_z during the frequency scans (a) without and (b) with 40 mTorr of He buffer gas. Due to the gravity, the particle is situated slightly below the central plane of the QIT. In both simulations, the initial positions and velocities of the particles were set at ($x_0 = 0$, $\upsilon_{x,0} = 0$), ($y_0 = 0$, $\upsilon_{y,0} = 0$) and ($z_0 = 1$ mm, $\upsilon_{z,0} = 0.01$ m/s), respectively, with a frequency-scan rate of 70 Hz/s over the range of 450–100 Hz.

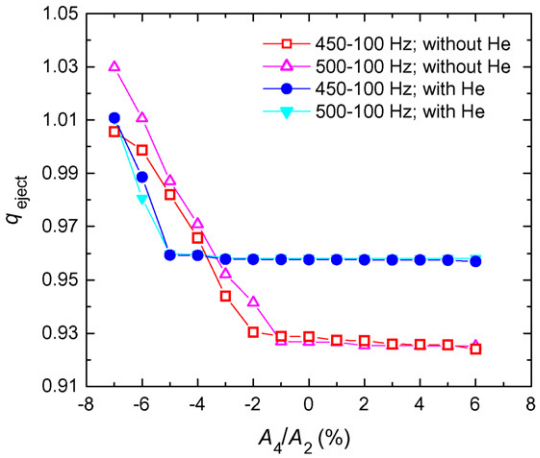

Fig. 8. Dependence of theoretically simulated q_{eject} on the percentage (A_4/A_2) of the octopole field relative to the basic quadrupole field in the nonlinear ion trap. The data points were obtained at two different frequency-scan ranges (as indicated) with and without 40 mTorr of He buffer gas. In all simulations, the initial positions and velocities of the particles were set at ($x_0 = 0$, $\upsilon_{x,0} = 0$), ($y_0 = 0$, $\upsilon_{y,0} = 0$) and ($z_0 = 1$ mm, $\upsilon_{z,0} = 0.01$ m/s), respectively, and the frequency-scan time was 5 s.

In Fig. 8, we also show the dependence of q_{eject} on A_4/A_2 over a wider range under the same initial conditions as described in Fig. 7. In the presence of 40 mTorr of He buffer gas, the q_{eject} value is quite stable; it increases only slightly (<0.005) when A_4/A_2 changes its polarity and magnitude from +6% to −5%. The value is also insensitive to the change of the frequency-scan range from 450–100 Hz to 500–100 Hz. However, a substantial increase in q_{eject} by more than 0.02 unit occurs between $A_4/A_2 = -5\%$ and −6%. Fig. 9 shows the trajectories of the particle's motion near the turning point at A_4/A_2 of −4%, −5% and −6%. There is no obvious difference in the trajectory between the cases of $A_4/A_2 = -4\%$ and −5%, where the amplitude of the particle's oscillatory motion displays a simple exponential increase in time near the particle ejection point (Fig. 9a and b). However, at $A_4/A_2 = -6\%$, slight modulation of the oscillation amplitude (Fig. 9c) carries the particle beyond the ejection point, resulting in a significant increase in q_{eject}. The behavior is very similar to the variation of z with q_z for the particle confined in the ion trap in the absence of buffer gas at $A_4/A_2 = -3\%$ as shown in Fig. 7a. In the latter case, the turning point is located at around −2% or −3%, depending on the frequency-scan range (Fig. 8).

As in the voltage scan [15], the finite scan time can also cause an ejection delay in the particle detection during the frequency-scan process. Fig. 10 shows the result of the simulations under various initial conditions with $x_0 = 0$, $\upsilon_{x,0} = 0$, $y_0 = 0$, $\upsilon_{y,0} = 0$, $-1 \le z_0 \le 1$ mm and $-0.01 \le \upsilon_{z,0} \le 0.01$ m/s at the rates of 35 Hz/s, 70 Hz/s, 140 Hz/s, 250 Hz/s and 350 Hz/s. The CV of the simulated q_{eject} values was found to increase substantially with the scan rate. Moreover, at higher scan rates such as 350 Hz/s, the location of the ejection point is very sensitive to the change of the initial conditions of the ions even in the presence of 40 mTorr of He buffer gas. Both of the characteristics are in good agreement with experimental observations, suggesting that the larger fluctuations in q_{eject} at higher frequency-scan rates as experimentally observed in Fig. 3 are predominantly

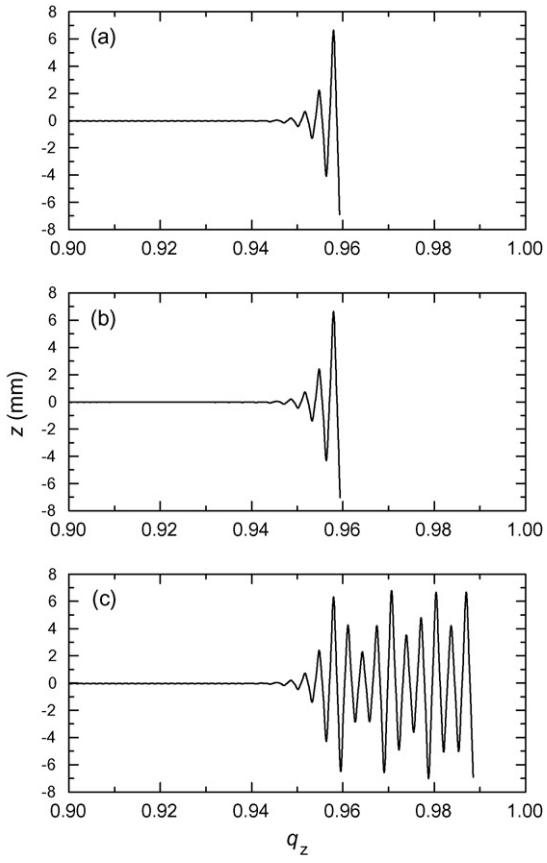

Fig. 9. Variations of the particle position z with the trap parameter q_z during the frequency scans of the quadrupole ion trap with (a) $A_4/A_2 = -4\%$, (b) $A_4/A_2 = -5\%$ and (c) $A_4/A_2 = -6\%$ near the particle ejection point in the presence of 40 mTorr of He buffer gas. In all simulations, the initial positions and velocities of the particles were set at ($x_0 = 0$, $\upsilon_{x,0} = 0$), ($y_0 = 0$, $\upsilon_{y,0} = 0$) and ($z_0 = 1$ mm, $\upsilon_{z,0} = 0.01$ m/s), respectively, with a frequency-scan rate of 70 Hz/s over the range of 450–100 Hz.

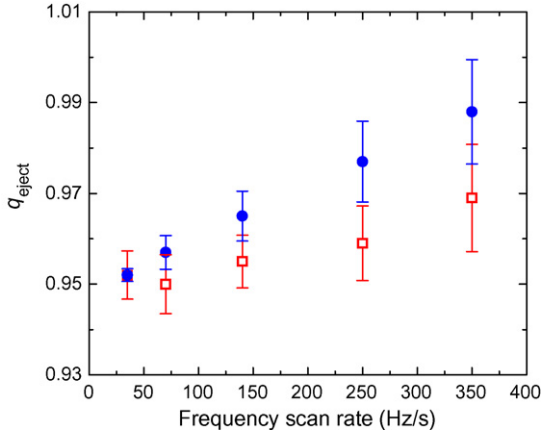

Fig. 10. Dependence of theoretically simulated q_{eject} on the frequency-scan rate with (●) and without (□) 40 mTorr of He buffer gas. The data points in each scan rate were obtained with initial positions and velocities of ($x_0 = 0$, $\upsilon_{x,0} = 0$) and ($y_0 = 0$, $\upsilon_{y,0} = 0$) in the x and y coordinates and various conditions of $z_0 = 0$, ±0.1, ±0.5, ±1.0 mm and $\upsilon_{z,0} = 0$, ±0.001, ±0.005, ±0.01 m/s in the z coordinate. Each error bar represents the coefficient of variance of the simulated q_{eject} values at each frequency.

contributed by the differences in the initial positions and velocities of the charge particles in the trap. To reduce this undesired effect, choice of lower scan rates as in mass analysis of small ions [3–5] is a necessity. Simultaneously, one should use buffer gas to damp the particles into the trap center so that the same initial conditions can be maintained. The trade-off is that an additional ejection delay is produced by the buffer gas damping effect (Fig. 10).

The simulation results depicted in Fig. 10 predict a near linear increase of q_{eject} with the frequency-scan rate, which is consistent with our experimental observations (Fig. 3). Such an effect is significant and can be substantial if the rate is too high. It suggests that re-calibration of the frequency-scan QIT mass spectrometer is needed whenever the scan rate is changed. At the scan rate of 70 Hz/s, as typically used in this and previous experiments [17], the q_{eject} values obtained by the simulations are 0.957 and 0.950 for the scans conducted in the presence and absence of 40 mTorr of He buffer gas, respectively. They agree satisfactorily with our experimental measurements of $q_{eject} = 0.952$ and 0.947, the mean values obtained from Fig. 2.

4. Conclusion

We have demonstrated that the combined technique involving frequency scan of a quadrupole ion trap operating in the mass-selective axial instability mode and charge detection of the ejected particles is a promising approach for high-speed mass analysis of micron-sized particles. The operation is realized by the availability of stable ac power amplifiers that allow smooth sweep of the trap driving frequency at constant voltage amplitude in the audio frequency region. Using 3-μm NIST polystyrene size standards as the mass calibrant, we have achieved a resolution of ∼100 and a measurement accuracy of ∼1% at m/z in the range of 10^9. The results are supported by theoretical simulations based on the generalized nonlinear Mathieu equations. The spectrometer so constructed is expected to find useful applications to a variety of biological cells and synthetic particles (either organic or inorganic), where knowledge of their total dry masses and dry mass distributions is in need.

References

[1] W. Paul, H.P. Reinhard, U. Von Zahn, Z. Phys. 152 (1958) 143.
[2] R.F. Wuerker, H. Shelton, R.V. Langmuir, J. Appl. Phys. 30 (1959) 342.
[3] R.E. Kaiser, R.G. Cooks, G.C. Stafford Jr., J.E.P. Syka, P.H. Hemberger, Int. J. Mass Spectrom. Ion Processes 106 (1991) 79.
[4] J.C. Schwartz, J.E.P. Syka, I. Jardine, J. Am. Soc. Mass Spectrom. 2 (1991) 198.
[5] F.A. Londry, G.J. Wells, R.E. March, Rapid Commun. Mass Spectrom. 7 (1993) 43.
[6] E.J. Davis, Aerosol Sci. Tech. 26 (1997) 212.
[7] W.-P. Peng, Y. Cai, H.-C. Chang, Mass Spectrom. Rev. 23 (2004) 443.
[8] M.A. Philip, F. Gelbard, S. Arnold, J. Colloid Interface Sci. 91 (1983)507.
[9] S. Schlemmer, J. Illemann, S. Wellert, D. Gerlich, J. Appl. Phys. 90 (2001) 5410.
[10] W.-P. Peng, Y.-C. Yang, M.-W. Kang, Y.T. Lee, H.-C. Chang, J. Am. Chem. Soc. 126 (2004) 11766.
[11] W.-P. Peng, Y.-C. Yang, C.-W. Lin, H.-C. Chang, Anal. Chem. 77 (2005) 7084.
[12] W.-P. Peng, Y.-C. Yang, M.-W. Kang, Y.-K. Tzeng, Z.X. Nie, H.-C. Chang, W. Chang, C.-H. Chen, Angew. Chem. Int. Ed. 45 (2006) 1423.
[13] A.J. Trevitt, P.J. Wearne, E.J. Bieske, Int. J. Mass Spectrom. 262 (2007) 241.
[14] Y. Cai, W.-P. Peng, S.-J. Kuo, Y.T. Lee, H.-C. Chang, Anal. Chem. 74 (2002) 232.
[15] Y. Cai, W.-P. Peng, S.-J. Kuo, H.-C. Chang, Int. J. Mass Spectrom. 214 (2002) 63.
[16] W.-P. Peng, H.-C. Lin, H.-H. Lin, M.-L. Chu, A.L. Yu, H.-C. Chang, C.-H. Chen, Angew. Chem. Int. Ed. 46 (2007) 3865.
[17] Z.X. Nie, F.P. Cui, Y.-K. Tzeng, H.-C. Chang, M. Chu, H.-C. Lin, C.-H. Chen, H.-H. Lin, A.L. Yu, Anal. Chem. 79 (2007) 7401.
[18] R.E. March, R.J. Hughes, Quadrupole Storage Mass Spectrometer, Wiley, New York, 1989.
[19] U.P. Schlunegger, M. Stoekli, R.M. Caprioli, Rapid Commun. Mass Spectrom. 13 (1999) 1792.
[20] Y. Cai, W.-P. Peng, H.-C. Chang, Anal. Chem. 75 (2003) 1805.
[21] W.-P. Peng, Y. Cai, Y.T. Lee, H.-C. Chang, Int. J. Mass Spectrom. 229 (2003) 67.
[22] L. Ding, M. Sudakov, S. Kumashiro, Int. J. Mass Spectrom. 221 (2002) 117.
[23] L. Ding, M. Sudakov, F.L. Brancia, R. Giles, S. Kumashiro, J. Mass Spectrom. 39 (2004) 471.
[24] L. Ding, S. Kumashiro, Rapid Commun. Mass Spectrom. 20 (2006) 3.
[25] L. Ding, F.L. Brancia, Anal. Chem. 78 (2006) 1995.
[26] D.E. Goeringer, W.B. Whitten, J.M. Ramsey, S.A. McLuckey, G.L. Glish, Anal. Chem. 64 (1992) 1434.
[27] W.B. Whitten, P.T.A. Reilly, J.M. Ramsey, Rapid Commun. Mass Spectrom. 18 (2004) 1749.
[28] M. Sudakov, Int. J. Mass Spectrom. 206 (2001) 27.
[29] G. Hars, Z. Tass, J. Appl. Phys. 77 (1995) 4245.
[30] J.P. Carrico, Dyn. Mass. Spectrom. 3 (1972) 1.
[31] H. Kahler, B.J. Lloyd Jr., Science 114 (1951) 34.
[32] J. Ting, EDN 46 (2001) 136.
[33] W.-P. Peng, Y.T. Lee, J.W. Ting, H.-C. Chang, Rev. Sci. Instrum. 76 (2005) 023108.
[34] A. Müller, Ann. Phys. 7 (1960) 6.
[35] Y. Wang, J. Franzen, Int. J. Mass Spectrom. Ion Processes 112 (1992) 167.
[36] Y. Wang, J. Franzen, K.P. Wanczek, Int. J. Mass Spectrom. Ion Processes 124 (1993) 125.
[37] J. Franzen, Int. J. Mass Spectrom. Ion Processes 125 (1993) 165.
[38] Y. Wang, J. Franzen, Int. J. Mass Spectrom. Ion Processes 132 (1994) 155.
[39] N.R. Whetten, J. Vac. Sci. Technol. 11 (1974) 515.
[40] T. Hasegawa, K. Uehara, Appl. Phys. B 61 (1995) 159.
[41] B.E. Dahneke, Aerosol Sci. 4 (1973) 147.